applied optics

Knife-edge interferogram analysis for corrosive wear propagation at sharp edges

ZHIKUN WANG† AND CHABUM LEE*,†

J. Mike Walker '66 Department of Mechanical Engineering, Texas A&M University, 3123 TAMU, College Station, Texas 77843-3123, USA
**Corresponding author: cblee@tamu.edu*

Received 16 December 2020; revised 12 January 2021; accepted 15 January 2021; posted 19 January 2021 (Doc. ID 417572); published 9 February 2021

This paper presents a novel noncontact measurement and inspection method based on knife-edge diffraction theory for corrosive wear propagation monitoring at a sharp edge. The degree of corrosion on the sharp edge was quantitatively traced in process by knife-edge interferometry (KEI). The measurement system consists of a laser diode, an avalanche photodiode, and a linear stage for scanning. KEI utilizes the interferometric fringes projected on the measurement plane when the light is incident on a sharp edge. The corrosion propagation on sharp edges was characterized by analyzing the difference in the two interferometric fringes obtained from the control and measurement groups. By using the cross-correlation algorithm, the corrosion conditions on sharp edges were quantitatively quantified into two factors: lag and similarity for edge loss and edge roughness, respectively. The KEI sensor noise level was estimated at 0.03% in full scale. The computational approach to knife-edge diffraction was validated by experimental validation, and the computational error was evaluated at less than 1%. Two sets of razor blades for measurement and control groups were used. As a result, the lag will be increased at an edge loss ratio of 1.007/μm due to the corrosive wear, while the similarity will be decreased at a ratio of 5.4×10^{-4}/μm with respect to edge roughness change. Experimental results showed a good agreement with computational results.

https://doi.org/10.1364/AO.417572

1. INTRODUCTION

Metal surface corrosion is a typical material damage process involving the deterioration of metal parts caused by the chemical effect in the presence of oxygen and water. The rate of corrosion on the metal surfaces increases with increasing temperature and increasing contents of C, N, P, and S [1]. Beginning long ago, corrosion has become the primary concern in various industry sectors such as the natural gas and oil industry, and the shipbuilding, machine tool, turbomachinery, and aerospace industries because of safety issues. Corrosion is a too costly problem in many applications. Damage resulting from corrosion lowers the mechanical and material properties of metal parts. Although metal or polymeric coatings help prevent erosion, those methods could not be an ultimate solution. Scheduling-based maintenance by vision inspection is the most common method to avoid corrosion issues on metal surfaces, but this method is limited to small-area inspection and does not allow for continuous metal surfaces monitoring. Thus, the industry is looking for low-cost monitoring and prediction technology to prevent catastrophic problems in advance due to the corrosion effect. There are two main reasons why corrosion propagation is difficult to predict and model: unstable slow corrosion rates and unpredicted results. The corrosion rate varies with many aspects: ambient environment, surface deformation, and fluid flowing rate; all of them will affect the corrosion rate. Moreover, the corrosion area on a specific structure is also hard to predict since it may happen anywhere in the structure. However, most of the commercially available corrosion measurement systems are designed for postprocessing, so the parts to be measured should be individually taken apart from whole systems, and the sample targets compatible with those measuring instruments are mostly planar. There are few methods to in-process enable monitoring and prediction of corrosion development.

A majority of research on corrosion monitoring and prediction have primarily focused on postprocessing to characterize the corrosion development from the planar metal surfaces by ultrasonics, radiography, optical fiber, microscopy, and surface profilers [2–12]. Those methods track the corrosion propagation in various structures such as pipelines, plate surfaces, and pipe walls, primarily focusing on uniform etch and pitting corrosion. However, sharp edges and corners of metal parts, for example, propellers in a boat engine, turbomachinery, or airplane engine, are also vulnerable to the corrosion process. Although those parts are coated or surface-treated against humidity, high temperature, and saltwater, those methods cannot permanently prevent rust from building up on sharp and corner edges. The corrosion issues on sharp edges always exist because corrosion could cause crack initiation and accelerate

mechanical part wear due to a dramatic increase in mechanical stresses at the sharp edges or corners.

Despite continuous research efforts, corrosion continues to present challenges, and there exists a knowledge gap in understanding corrosion propagation in microscale or nanoscale processes in certain environmental conditions [13]. Technological investigation microscale or nanoscale corrosion science enables us to understand and predict corrosion initiation and progress mechanisms. Such efforts would detect corrosion initiation before corrosion processes initiate. Because edges and corners of the metal surface are more sensitively reactive to corrosion than the planar surfaces [14,15], microscale or nanoscale corrosion measurement techniques capable of corrosion propagation and its characterization at the edges or corners must have a significant impact on infrastructure and industry.

Although the work of finding the best solution for edge monitoring never stops, all these methods have more or fewer problems. There are some investigations for corrosion inspection systems, but they just focus on the corrosion effect for the surface conditions. Also, the profile for the sharp edges can be traced by many methods such as the microscope, SEM, and AFM, but they all perform the measurement in the same way asconventional postprocessing. For those methods, the sharp edge needs to be removed from the manufacturing system, and thus the working process must be paused. Currently, there exist no instruments for corrosion propagation monitoring in sharp edges *in situ* and real time. Based on the reasons above, industries need a novel method to track the corrosion propagation along the sharp edges in real time for workpiece quality control and system maintenance. Fortunately, knife-edge diffraction can satisfy all the requirements above.

Recently, many approaches to dimensional measurements by utilizing the diffraction phenomenon at the shape edges, the so-called knife-edges, have appeared. Knife-edge diffraction is a phenomenon first proposed by Foucault in 1856 [16], and its principle could be explained by geometrical optics. In 1961, Keller summarized his work from former researchers [17]. When light propagates where no particles are present in the free space and passes partially through the sharp edge, a portion of the light will be blocked, and others will just propagate in the free space. The diffracted rays can be viewed as ordinary rays that come from the Huygens wavelet generated by the blocked incident rays on the edge boundary. The light interference between the blocked and unblocked lights takes place. Now, with the phase difference from the original rays and the diffracted rays, the light will change with the area blocked by the sharp edge changes due to the alternating constructive or destructive interference between original rays and diffracted rays. Therefore, a fringe pattern can be generated. Since the diffracted rays are generated on the edge, we can estimate the edge profile by tracking the recorded knife-edge diffraction fringe pattern. Lee *et al*. utilized the knife edge for optical metrology and developed knife-edge interferometry (KEI) techniques for displacement sensing [18–22], cutting tool condition monitoring [22–24], and motion error measurements [25]. Korneev *et al*. [26] demonstrated an experiment using a knife edge for producing partial interferograms and observed that the interferograms correspond to the knife-edge orientation. Xochihuila *et al*. [27] used the KEI for testing concave lenses with a collimated beam.

In this study, a new measurement method based on knife-edge diffraction theory is proposed to allow for in-process, low-cost, convenient corrosion monitoring at the sharp edges so the corrosion rates of sharp edges could be characterized. This study will help predict the corrosion status and life cycle of metal parts. The measurement principle, measuring system design, and experiment results are discussed below.

2. MEASUREMENT PRINCIPLE

The measurement principle of the KEI system for the measurement and inspection of corrosive wear propagation, as depicted in Fig. 1, is based on the edge diffraction theory [28]. For instance, when the sharp edge (e.g., a razor blade) is lightened by a light source such as a laser diode and is scanned along the perpendicular direction, based on the Huygens–Fresnel principle [29], the shining area on the razor blade can be viewed as a Huygens wavelet, which can be represented as a point light source in an optical system. In that case, the original beam will interfere with the point light source scattered at the edge, and the diffraction signal can be recorded by the photodiode. Assuming a laser beam transmitted into the system with a diameter of a, a razor blade is placed perpendicular to the optical axis at the right side of the laser diode. The light intensity sensor is placed along the optical axis at the right side of the razor blade. Now the light intensity on the sensor can be calculated by the Fresnel diffraction equation [30] as

$$U_0(r_0) = \frac{-je^{jkz_0}}{\lambda z_0} \int_{-\frac{a}{2}}^{\frac{a}{2}} e^{\frac{jk}{2z_0}(x_0-x_s)^2} \mathrm{d}x_s \int_{-\frac{a}{2}}^{\frac{a}{2}} e^{\frac{jk}{2z_0}(y_0-y_s)^2} \mathrm{d}y_s. \tag{1}$$

Here, j is the expression of the imaginary part, k $(2\pi/\lambda)$ is the wavenumber, λ is the wavelength of the laser diode, and z_0 is the distance between the razor blade and the sensor. Also, x_o and y_o imply the positions of the light intensity sensor, while x_s and y_s show the point on the cross section of the laser beam at the plane of the sharp edge for integration. The simulation results of edge diffraction with respect to parameter changes are shown in Fig. 2, where ⊘ indicates the diameter of the laser beam, and L is the optical distance between the knife edge and the detector.

Figure 2 shows the knife-edge interferometric fringe patterns according to three parameter changes. Here the detector size was considered to be infinitely small as a point on the optical axis. However, the detector size could introduce the difference between the simulation result and the actual fringe pattern. In real experiment data recording, the detector has its own effective sensing area. The actual light intensity was integrated over the effective sensing area and normalized. The simulation result, including the effective sensing area effect, is added in Fig. 3. In this simulation, the detector diameter equals to 100 μm, which is the effective sensing area of the photodiode used in the experiment.

Although the knife-edge diffraction was well studied many years ago, newer experimental approaches and applications have recently been introduced by Lee [16–18]. Lee proposed a new parameter that can be introduced into the knife-edge diffraction theory for real-life applications: edge roughness

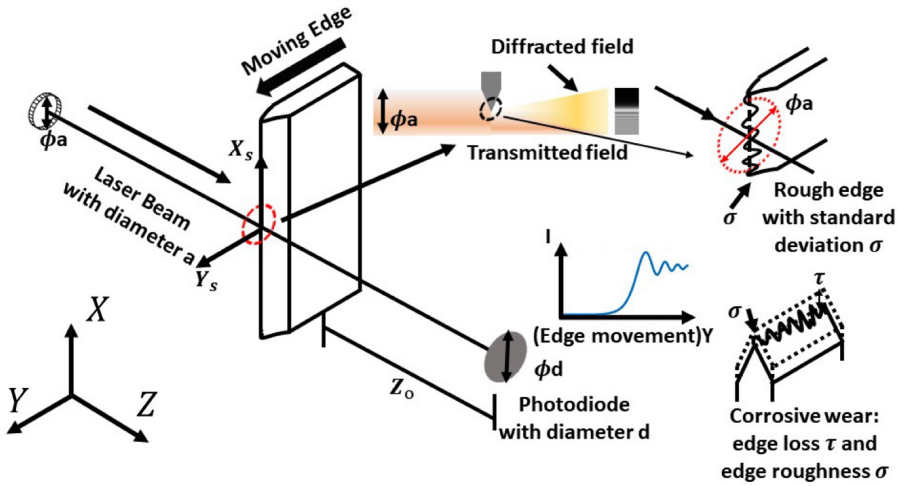

Fig. 1. Schematic of the principle edge diffraction theory. The beam is partially blocked by a razor blade; the gold area is the light field diffracted by the edge, while the orange field is the transmitted field from laser beam. ϕa and ϕd are the diameter of the laser beam and photodiode, x_s implies the x coordinate of the point in laser beam, y_s is the y coordinate of the point in the laser beam, Z_0 is the distance from the edge to the photodiode, σ is the standard deviation of the edge roughness in the Gaussian PDF, and τ is the edge loss on the edge.

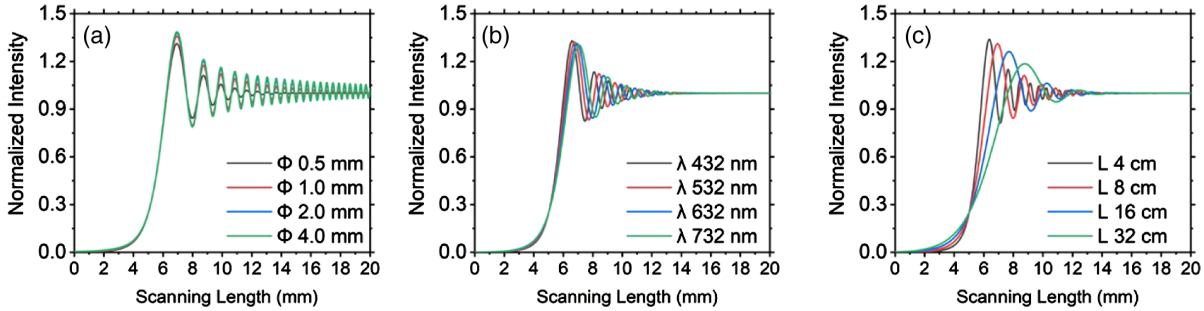

Fig. 2. Fresnel diffraction simulation results with respect to (a) beam diameter, (b) wavelength, and (c) optical distance between the edge and the detector.

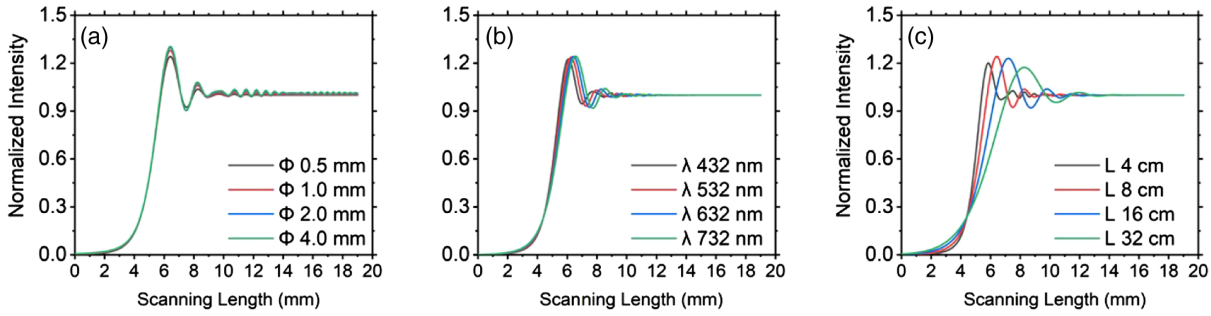

Fig. 3. Fresnel diffraction simulation result (effective sensing area 100 μm) with respect to (a) beam diameter ø, (b) wavelength λ, and (c) optical distance L between the edge and the detector.

characterization, displacement sensing, and tool condition monitoring. In this theory, the knife-edge boundary profile is assumed to satisfy the Gaussian probability density function (PDF), and the roughness only distributes along the axis that is perpendicular to the light transaction. In that case, the Huygens wavelet generated on the edge will not transmit light to the ambient area uniformly. In other words, the light will be scattered randomly due to its rough edge profile Δh. The deviated fringe pattern can be mathematically formulated by adding a PDF term form with standard deviation σ as a function of edge topography into the Fresnel diffraction [17], that is,

$$\mathrm{PDF}(\Delta h) = \frac{1}{\sqrt{2\pi}\sigma} e^{-\frac{\Delta h^2}{2\sigma^2}}. \tag{2}$$

Thus, the edge diffraction effect on the edge roughness can be expressed as [17]

$$U_0(r_0) = \frac{-je^{jkz_0}}{\lambda z_0} \int_{-\frac{a}{2}}^{\frac{a}{2}} e^{\frac{jk}{2z_0}(x_0 - x_s)^2} \mathrm{d}x_s \times \int_{-\frac{a}{2}}^{\frac{a}{2}} e^{\frac{jk}{2z_0}(y_0 - y_s)^2} \frac{1}{\sqrt{2\pi}\sigma} e^{-\frac{\Delta h^2}{2\sigma^2}} \mathrm{d}y_s. \tag{3}$$

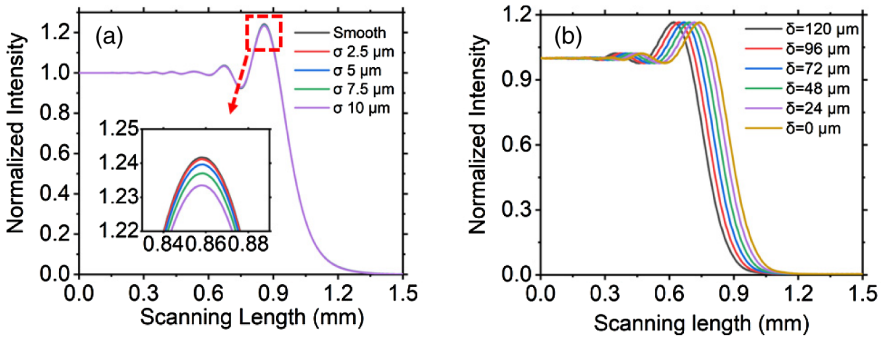

Fig. 4. Fringe patterns for verification. (a) Fringe pattern with different edge roughness from 0 to 10 μm, and (b) fringe pattern with different edge loss from 0 to 120 μm.

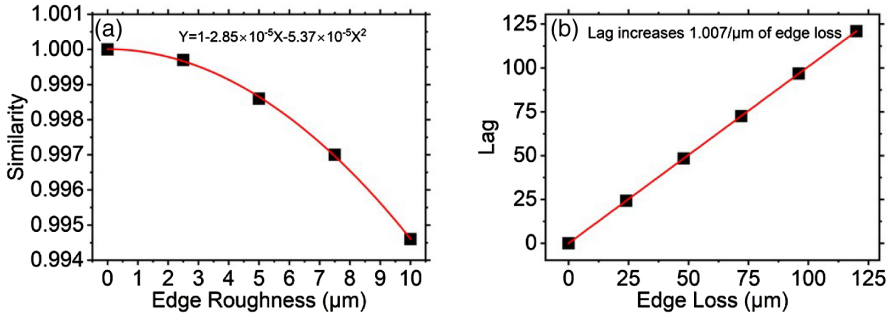

Fig. 5. Analysis results. (a) Similarity changes as edge roughness increases, and (b) lag changes as edge loss increases.

Now the intensity distribution of the diffraction can be used as evidence to expose the changes in edge roughness.

To determine the topography conditions of the sharp edge, the KEI signals can be analyzed by the cross-correlation method [22]. Cross correlation can track the similarity and lag of two data sets as a function of displacement of one relative to another. In this study, this method was employed to characterize the edge roughness and the material loss of the sharp edges. The outputs of cross correlation of two data sets are the lag presenting macrocorrosive wear and the lag representing microcorrosive wear. Macrocorrosive wear represents the critical corrosive wear changing the dimensions of the sharp edges. On the other hand, microcorrosive wear indicates the roughness on the sharp edges and causes the interference loss because of the inherence of the diffracted light at the sharp edges. Thus, the lag and similarity of cross correlation could be a result of macro- and microcorrosive wear of the sharp edges, respectively. While analyzing the data, the cross correlation for measurement group data and control group data in day one will be utilized as a reference to calculate the similarity. The similarity can be calculated by comparing the cross-correlation result between one day and another. By using the similarity and lag calculated from the cross-correlation function available from MATLAB and the algorithm developed by Svilainis [31], the corrosion effect on sharp edges can be characterized.

To implement the cross-section method for corrosive wear measurement, we derived two groups of simulation data for confirmation. Figure 4 shows the plot of the fringe pattern for verification. In Fig. 4(a), we generated the fringe pattern with different edge roughness information for similarity confirmation, while Fig. 4(b) implies the fringe pattern with different edge corrosive loss for lag verification. The result of the simulation can be seen in Fig. 5. Figure 5(a) shows the result of similarity changes with respect to edge roughness changes. As the 10 μm edge roughness increases, the razor blade's similarity decreases from 1.000 to 0.9945. In Fig. 5(b), the relationship between the lag and the corrosive edge loss is generated. Six groups of data with edge loss increment (every 24 μm) was applied into the script to calculate the lag for each group. After the data analysis by the script, the lag increases as the loss-induced fringe pattern changes increase. The analysis result of those generated data can be seen in Fig. 5(b). The actual edge loss for group 5 was 120 μm, while the calculated edge loss was 120.9287 μm. The error rate was estimated to be 0.8%.

3. EXPERIMENT

A prototype KEI system was constructed to explore the corrosion phenomenon on the sharp edge (razor blade). The whole experiment setup consists of a laser diode (λ 633 nm), an aperture (ϕ 1 mm), a precision linear stage for scanning, two razor blades, an avalanche photodiode (APD), hydrochloride acid (concentration about 36.5%–38.0%). The schematic of the experiment setup and the real system can be seen in Fig. 6. A well-aligned laser diode was placed at the right side in the system generating the laser beam passing through an aperture. Two sets of razor blades were securely fixed on the precision linear scanning stage for the experiment as a measurement group and a control group. At the end of the system, a light intensity sensor made by the APD was placed strictly parallel to the optical axis. A microscope (200×) was located at the same height as the light intensity sensor for edge profile collection purposes. During the

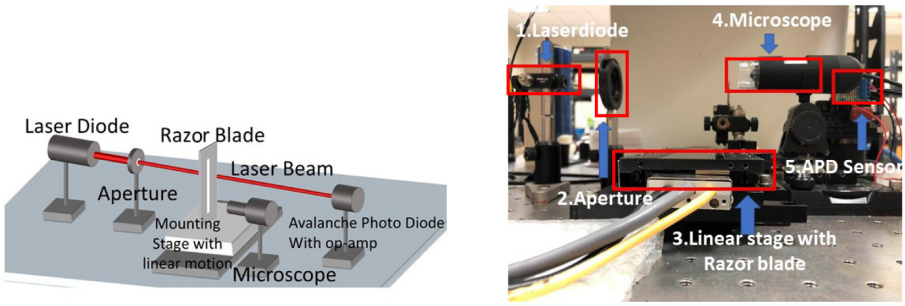

(a) (b)

Fig. 6. Experimental setup. (a) Schematic of experiment setup, and (b) prototype of experiment setup. (1) Laser diode was placed at the left side of the experiment setup for light supply. (2) The aperture was placed at the right of the laser diode to constrain the diameter of the laser diode. (3) The linear stage with razor blades was placed in the middle to generate the laser blocking motion. (4) The microscope was placed at the right side for edge picture recording. (5) The APD sensor was placed at the end for light intensity recording.

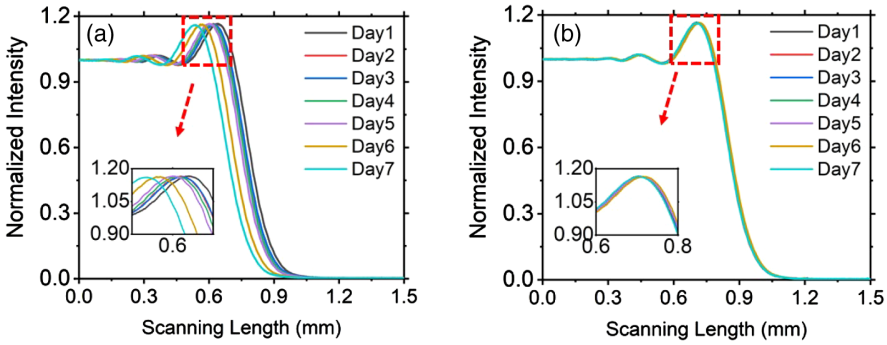

Fig. 7. Fringe patterns. (a) Measurement and (b) control group.

experiment, the razor blade from the measurement group will be rinsed with hydrochloride acid every day for corrosion purposes [32]. Meanwhile, the razor blade in the control group will be isolated to keep the natural condition as a comparison. When the hydrochloride dries out, the laser beam will pass through two razor blades separately to generate the fringe patterns. Those groups of data will be recorded by the National Instruments data acquisition card with an acquisition rate of 100 kHz. Three sets of data per day for each group were recorded to avoid the occasional error. The recorded fringe can be seen in Fig. 7.

The developed instrument *in situ* measures the corrosion conditions. If the sample is detached for the postprocessing to validate the work, the optical alignment will change, which means that the initial condition information of the corrosion will be lost. Thus, the experiment was performed without detaching the measurement samples, but the proper measurement methods were used for the validation.

The recorded data were analyzed using the cross-correlation method. Fringe patterns were tracked over 1.5 mm. By comparing the similarity from Day 1 to Day 7, the extent of edge roughness was monitored. Similarity and lag results for seven days are shown in Fig. 8. Here, the similarity values overall decreased from Day 1 to Day 7, and the decrease of 0.0068 implies the 10.99 μm edge roughness changes due to the corrosive wear, which was calculated from the relationship [Fig. 5(a)]. From Fig. 8(b), the lag changes 105.73 from Day 1 to Day 7 in the measurement group, which equals to 105.21 μm of corrosive edge loss happening on the edge. While analyzing the data, the noise level should also be considered. To determine the noise level of the KEI system, the error that needs to be considered is the noise in data recording. During the data recording process, the standard deviation of the data recorded by photodiode is 0.00089 V (0.03 % sensor noise in full scale).

The test sample will lose its initial position when the sample is relocated for postprocess measurement. The reference distance marked on the measurement sample was measured to estimate the corrosive edge loss without detaching the knife edge. Thus, the validation process was performed on-machine. The razor blade has a hole in the middle. When the test sample was scanned, the laser passed through the hole and the knife-edge area. As seen in Fig. 9, the laser light was blocked within the distance d when the razor blade was scanned by the precision linear stage moving in a constant speed v. The distance d can be calculated by multiplying the time Δt and the scanning speed v. Here, the distance d was measured as corrosive wear taking place for 7 days. The change of the distance d can be considered as corrosive edge loss. As seen in Fig. 9(b), the corrosive edge loss calculated from the cross correlation and the validation method [Fig. 9(a)] showed good agreement.

We also took pictures of each razor blade every day by using a portable optical microscope for corrosive wear monitoring validation. The edge profile for two razor blades from Day 1 to Day 7 can be seen in Fig. 10. As a result, it can be considered that the proposed edge corrosion monitoring system can be utilized for corrosion propagation monitoring of the sharp edge.

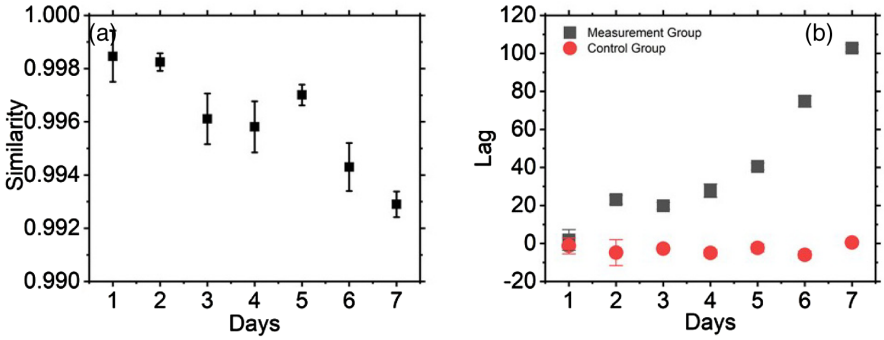

Fig. 8. Experimental results. (a) Similarity and (b) lag.

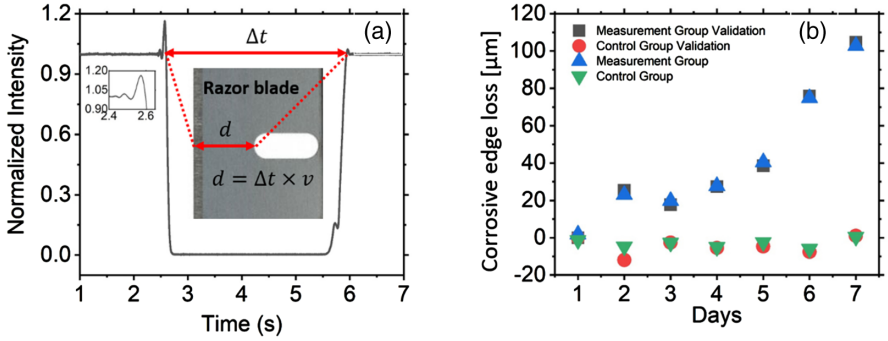

Fig. 9. Experimental validation results. (a) Validation process and (b) comparison.

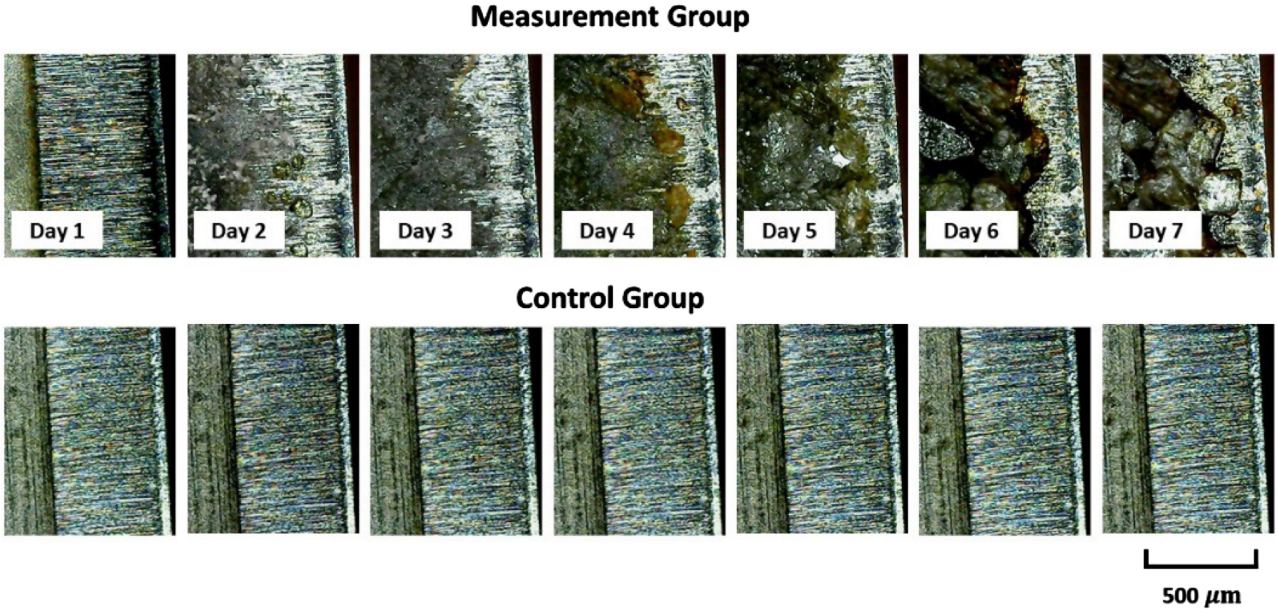

Fig. 10. Edge images for measurement and control groups.

4. CONCLUSION

This study introduced a low-cost and novel sensing method for sharp edge corrosion monitoring based on edge diffraction, and the theoretical model enabling corrosive wear quantification was developed. The computational results showed a good agreement with experimental results. The KEI sensor noise level was estimated to be 0.03% in full scale. Based on the proposed measurement principle, two types of edge defects could be determined: edge roughness and edge loss. There has been no previous study reported about noncontact corrosive edge monitoring, to the best of our knowledge. The scanning electron microscopy or atomic force microscopy could be used, but those are for postprocessing. The proposed method could in-process measure, characterize, and monitor the corrosive wear propagation. Our next step is to increase the resolution of the knife-edge interference system by signal processing and

optics modeling available for real manufacturing systems for commercial use. The ability of edge roughness monitoring can also be optimized because the similarity only changes 0.005 with 10-μm standard deviation of edge roughness PDF added. It is expected that this technique can be used for health monitoring and maintenance of impellers, propellers, or blades, astheir edge quality and conditions are critical for their performance in the near future.

Funding. National Science Foundation (1855473).

Disclosures. The authors declare no conflicts of interest.

Data Availability. The data that support the findings of this study are available from the corresponding author upon reasonable request.

[†]All authors contributed equally to this work.

REFERENCES

1. E. Bardal, *Corrosion and Protection* (Springer, 2004), Chap. 8.
2. N. A. Rodríguez-Olivares, J. V. Cruz-Cruz, A. Gómez-Hernández, R. Hernández-Alvarado, L. Nava-Balanzar, T. Salgado-Jiménez, and J. A. Soto-Cajiga, "Improvement of ultrasonic pulse generator for automatic pipeline inspection," Sensors **18**, 2950 (2018).
3. F. Cegla, "Ultrasonic monitoring of corrosion with permanently installed sensors (PIMS)," in *Sensors, Algorithms and Applications for Structural Health Monitoring. IIW Collection*, B. Chapuis and E. Sjerve, eds. (Springer, 2018), pp. 13–20.
4. F. Lakestani, J.-F. Coste, and R. Denis, "Application of ultrasonic Rayleigh waves to thickness measurement of metallic coatings," NDT&E Int. **28**, 171–178 (1995).
5. K. Edalati, N. Rastkhah, A. Kermani, M. Seiedi, and A. Movafeghi, "The use of radiography for thickness measurement and corrosion monitoring in pipes," Int. J. Press. Vessel. Pip. **83**, 736–741 (2006).
6. M. Ghahari, D. Krouse, N. Laycock, T. Rayment, C. Padovani, M. Stampanoni, F. Marone, R. Mokso, and A. J. Davenport, "Synchrotron x-ray radiography studies of pitting corrosion of stainless steel: extraction of pit propagation parameters," Corros. Sci. **100**, 23–35 (2015).
7. G. Qiao, Z. Zhou, and J. Ou, "Thin Fe-C alloy solid film based fiber optic corrosion sensor," in *Proceeding of 1st IEEE International Conference on Nano/Micro Engineered and Molecular Systems*, Zhuhai, China, 18–21 January 2006.
8. Z. Pei, D. Zhang, Y. Zhi, T. Yang, L. Jin, D. Fu, X. Chen, H. A. Terryn, J. M. C. Mol, and X. Li, "Towards understanding and prediction of atmospheric corrosion of an Fe/Cu corrosion sensor via machine learning," Corros. Sci. **170**, 108697 (2020).
9. D. Saying, L. Yanbiao, T. Qian, L. Yanan, Q. Zhigang, and S. Shizhe, "Optical and electrochemical measurements for optical fibre corrosion sensing techniques," Corros. Sci. **48**, 1746–1756 (2006).
10. W. Dai, X. Wang, M. Zhang, W. Zhang, and R. Wang, "Corrosion monitoring method of porous aluminum alloy plate hole edges based on piezoelectric sensors," Sensors **19**, 1106 (2019).
11. D. Wang, W. Zhang, X. Wang, and B. Sun, "Lamb-wave-based tomographic imaging techniques for hole-edge corrosion monitoring in plate structures," Materials **9**, 916 (2016).
12. Y. He, "Wireless corrosion monitoring sensors based on electromagnetic interference shielding of RFID transponders," Corrosion **76**, 411–423 (2020).
13. S. C. Hayden, C. Chisholm, R. O. Grudt, J. A. Aguiar, W. M. Mook, P. G. Kotula, T. S. Pilyugina, D. C. Bufford, K. Hattar, T. J. Kucharski, I. M. Taie, M. L. Ostraat, and K. L. Jungjohann, "Localized corrosion of low-carbon steel at the nanoscale," npj Mater. Degrad. **3**, 17 (2019).
14. Y. Zhang, J. M. Lucas, P. Song, B. Beberwyck, Q. Fu, W. Xu, and A. P. Alivisatos, "Superresolution fluorescence mapping of single nanoparticle catalysts reveals spatiotemporal variations in surface reactivity," Proc. Natl. Acad. Sci. USA **112**, 8959–8964 (2015).
15. C. L. Bentley, M. Kang, and P. R. Unwin, "Nanoscale surface structure-activity in electrochemistry and electrocatalysis," J. Am. Chem. Soc. **141**, 2179–2193 (2019).
16. F. Zernike, "Diffraction theory of the knife-edge test and its improved form, the phase-contrast method," Mon. Not. R. Astron. Soc. **94**, 377–384 (1934).
17. J. B. Keller, "Geometrical theory of diffraction," J. Opt. Soc. Am. **52**, 116–130 (1962).
18. C. Lee, S.-K. Lee, and J. A. Tarbutton, "Novel design and sensitivity analysis of displacement measurement system utilizing knife-edge diffraction for nanopositioning stages," Rev. Sci. Instrum. **85**, 095113 (2014).
19. C. Lee, S.-K. Lee, and J. A. Tarbutton, "Positioning control effectiveness of optical knife-edge displacement sensor-embedded monolithic precision stage," Sens. Actuators A. **233**, 390–396 (2015).
20. C. Lee, C. K. Stepanick, S.-K. Lee, and J. A. Tarbutton, "Cross-coupling effect of large range XY nanopositioning stage fabricated by stereolithography process," Precis. Eng. **46**, 81–87 (2016).
21. C. Lee, S. M. Mahajan, R. Zhao, and S. Jeon, "A curved edge diffraction-utilized displacement sensor for spindle metrology," Rev. Sci. Instrum. **87**, 075113 (2016).
22. C. Lee, R. Zhao, and S. Jeon, "A simple optical system for miniature spindle runout monitoring," Measurement **102**, 42–46 (2017).
23. S. Jeon, C. K. Stepanick, A. A. Zolfaghari, and C. Lee, "Knife-edge interferometry for cutting tool wear monitoring," Precis. Eng. **50**, 354–360 (2017).
24. S. Jeon, A. Zolfaghari, and C. Lee, "Dicing wheel wear monitoring technique utilizing edge diffraction effect," Measurement **121**, 139–143 (2018).
25. C. Lee, S. Jeon, C. K. Stepanick, A. Zolfaghari, and J. A. Tarbutton, "Investigation of optical knife-edge sensor for low cost, large-range and dual-axis nanopositioning stages," Measurement **103**, 157–164 (2017).
26. N. Korneev, F. S. G. Agustín, P. C. Xochihuila, R. D. Uribe, and A. Cornejo-Rodríguez, "Optical testing with a knife-edge interferometer," J. Phys. Conf. Ser. **274**, 012063 (2011).
27. P. C. Xochihuila, N. K. Zabello, F. S. Granados-Agustín, J. R. Díaz-Uribe, and A. Cornejo-Rodríguez, "Knife-edge interferometer. Part I: with collimated beam," Opt. Eng. **53**, 092006 (2014).
28. E. Hecht, *Optics* (Addison-Wesley, 2002).
29. M. Born, E. Wolf, and E. Hecht, "Principles of optics electromagnetic theory of propagation, interference and diffraction of light," Phys. Today **53**, 77–78 (2000).
30. G. L. Clarke, "*Geometrical theory of diffraction for electromagnetic waves*," (Peter Peregrinus, UK1986).
31. L. Svilainis, "Review on time delay estimate subsample interpolation in frequency domain," IEEE Trans. Ultrason. Ferroelectr. Freq. Control **66**, 1691–1698 (2019).
32. M. Abdallah, "Rhodanine azosulpha drugs as corrosion inhibitors for corrosion of 304 stainless steel in hydrochloric acid solution," Corros. Sci. **44**, 717–728 (2002).